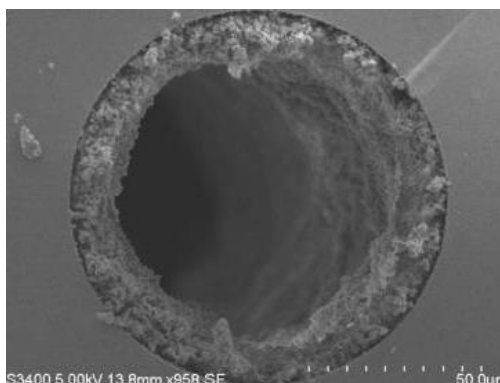


# Controlled Ultraviolet (UV) Photoinitiated Fabrication of Monolithic Porous Layer Open Tubular (monoPLOT) Capillary Columns for Chromatographic Applications

David A. Collins, Ekaterina P. Nesterenko, Dermot Brabazon, and Brett Paull

## ABSTRACT:

An automated column fabrication technique that is based on a ultraviolet (UV) light-emitting diode (LED) array oven, and provides precisely controlled “in-capillary” ultraviolet (UV) initiated polymerization at 365 nm, is presented for the production of open tubular monolithic porous polymer layer capillary (monoPLOT) columns of varying length, inner diameter (ID), and porous layer thickness. The developed approach allows the preparation of columns of varying length, because of an automated capillary delivery approach, with precisely controlled and uniform layer thickness and monolith morphology, from controlled UV power and exposure time. The relationships between direct exposure times, intensity, and layer thickness were determined, as were the effects of capillary delivery rate (indirect exposure rate), and multiple exposures on the layer thickness and axial distribution. Layer thickness measurements were taken by scanning electron microscopy (SEM), with the longitudinal homogeneity of the stationary phase confirmed using scanning capacitively coupled contactless conductivity detection (sC4D). The new automated UV polymerization technique presented in this work allows the fabrication of monoPLOT columns with a very high column-to-column production reproducibility, displaying a longitudinal phase thickness variation within  $\pm 0.8\%$  RSD (relative standard deviation).



## Introduction

Porous layer open-tubular capillary columns (PLOT) possess a porous layer of stationary phase covering the inner surface of the capillary tubing, preserving an open-tubular structure after the completion of all column preparation steps. Chromatographic separations on modern PLOT columns can result from various solute–sorbent interactions, in addition to simple partitioning, involving a wide variety of functionalized surfaces.

Over the past few decades, numerous PLOT columns have been developed and applied in many different areas of separation science. Open tubular (OT) columns were initially

proposed for gas chromatography (GC) by Golay<sup>1</sup> and, following this pioneering development, OT capillary GC has practically replaced packed-column GC for most analytical applications, with PLOT columns now well-established as a common OT column format.<sup>2</sup> Furthermore, electrophoretic methods, such as capillary zone electrophoresis (CZE), are predominantly OT capillary-based, with related techniques, such as capillary electrochromatography (CEC), having been developed using not only particle-packed and monolithic-type stationary phases, but also now commonly with PLOT columns.<sup>3-6</sup> In addition to the above techniques, the application of PLOT columns to microsolid phase extraction ( $\mu$ -SPE) has also been reported.<sup>7,8</sup>

As far back as the late 1970s, there have been attempts to apply OT format columns to liquid chromatographic (LC) separations,<sup>9-11</sup> although, in most early cases, practical and instrumental restrictions meant that only limited interest was generated. Over the past decade, most instrumental issues have been largely resolved, and sensitive small volume detectors, compatible with capillary format, together with gradient pumps capable of sub  $\mu$ L/min flow rates, have become readily available.

This has seen OT capillary-LC, and, in particular, the use of PLOT columns in LC attract considerable new attention. Indeed, recently, the use of PLOT capillary columns for high-efficiency and high-peak-capacity separations, coupled with mass spectrometric detection, in areas such as proteomics, has been reported by several leading groups.<sup>12-14</sup> In addition, recent studies into the optimal structures for PLOT columns in liquid chromatography for high-efficiency separations have also been reported.<sup>15</sup> One approach to produce the stationary phase within PLOT columns is to immobilize a thin layer (usually  $<10 \mu\text{m}$ ) of small particles to the inner surface of the capillary column.

This has been shown with metal oxides,<sup>16</sup> carbon, molecular sieves,<sup>2</sup> metal nanoparticles,<sup>17</sup> and various derivatives of styrene.<sup>7,18</sup> However, a potential disadvantage of this approach is the leaching or bleeding of particles from the wall over time, which affects not only the separation performance, but also may result in damage of detectors, especially mass spectrometers.

An alternative approach is the direct covalent attachment of a porous polymer layer to the inner surface of the capillary tubing. This type of stationary phase can provide a highly developed surface area, as required for chromatographic performance and capacity, and is also both physically and chemically stable, for example, being compatible with both basic and acidic buffer systems. In addition, the use of such porous polymeric stationary phases provides the substrate upon which surface chemistry can be relatively easily varied, through simple surface modification procedures, which can be carried out in situ. To date, the majority of PLOT columns produced, based on immobilization of a polymeric phase as a single porous layer (monolithic structure) onto the inner surface of the column tubing, have been obtained through the application of thermally initiated polymerization.<sup>14,5,6,19-22</sup>

It has been shown that, using thermal polymerization, PLOT columns of different dimensions (from an inner diameter (ID) of  $10-75 \mu\text{m}$  and lengths up to 3.2 m) can be produced, which

can then be functionalized with varying chemistries for use in LC applications, such as in reverse-phase LC (RP-LC),<sup>21</sup> hydrophilic interaction liquid chromatography (HILIC),<sup>22</sup> or for extraction applications, e.g., based on a molecular imprinted polymer (MIP)<sup>5</sup> or an immobilized ion-exchanger.<sup>6</sup> As an extension on the standard thermal polymerization approach, Xu and Sun<sup>23</sup> have also reported the fabrication of a tentacle-type polymer-modified OT column by glycidyl methacrylate (GMA) grafted polymerization, for further modification with various functional groups. However, for all of the above work, the biggest challenge when using thermal polymerization is the formation of a uniform polymer layer of desired thickness, with initiator concentration and polymerization time considered as critical factors for the optimization and reproducibility of the immobilization reaction. Kuban et al.<sup>24</sup> have presented one way to avoid such considerations, reporting the fabrication of polymer ion-exchange PLOT columns prepared using a layer-by-layer “cold” fabrication approach. In their work, an anionexchange PLOT column of relatively large bore (75- $\mu\text{m}$  ID) was prepared through layer-by-layer polycondensation of a primary amine with a diepoxide, namely, methylamine and 1,4-butanedioldiglycidyl ether. In this case, the resultant PLOT column was applied to low-pressure OT anion-exchange chromatography.

Recently, several research groups have presented PLOT columns produced by UV-initiated polymerization.<sup>3,25,26</sup> Eeltink et al.<sup>3</sup> prepared capillary columns with methacrylate ester-based monolithic-type porous polymer coatings via UV-initiated free-radical polymerization of butylmethacrylate and a cross-linker (ethylene dimethacrylate), using 1-octanol as a porogen. However, once again, it was shown that obtaining a uniform polymer layer is a nontrivial task. If the capillary filled with the polymerization mixture was placed under a UV light source, where it remained motionless during all the irradiation time, the resulting polymer coating was found to be nonuniform. Rotation of the capillary at 100 rpm during polymerization did result in the formation of a more uniform layer; however, the overall technique could only produce relatively short PLOT columns, restricted by the UV chamber dimensions. Abele et al.<sup>25</sup> recently introduced a novel evanescent wave (EW)-initiated photopolymerization technique, using a single light-emitting diode (LED) for the fabrication of monolithic PLOT columns.

The EW photopolymerization was induced by the evanescent field created at the inner wall of a transparent polytetrafluoroethylene-coated fused silica capillary illuminated axially and acting as a lightwaveguide. The authors proposed the resultant PLOT columns for use as capillary reactors, within nanoliquid chromatography (nano-LC), CEC, and related separation methods. It was shown that columns with a layer thickness ranging from 2  $\mu\text{m}$  to 25  $\mu\text{m}$  were obtained; however, again, only short columns (<11 cm) could be produced using this approach, as layer thickness would vary along the column length, decreasing with the increase of distance from the light source, because of attenuation within the silica medium. Following this work, Nesterenko et al.<sup>26</sup> reported the preparation of slightly longer monolithic porous layer open tubular (monoPLOT) columns using an automated UV scanning technique. In this work, capillaries filled with polymerization mixture were repeatedly exposed to light from the scanning source at a wavelength of 365 nm. The UV

source was moved along the length of the capillary column at a uniform scan rate and for an optimized length of time (up to 25 min).

The monolithic phase was formed during this perpendicular illumination. This method resulted in the fabrication of columns with a very uniform layer thickness which was confirmed using scanning capacitively coupled contactless conductivity detection (sC4D). However, using this method, it was only possible to produce columns as long as 30–40 cm. Therefore, it can be seen that the preparation of surfacebonded porous phases within open-tubular columns, of a uniform layer thickness and able to provide sufficient phase capacity for application within capillary-LC, still remains a considerable challenge. For this reason, and described herein, a novel automated capillary column UV polymerization technology for the fabrication of monoPLOT columns of variable length and phase thicknesses has been developed. A prototype feed-through UV curing oven was designed and built for this purpose. The system was tested in both static and dynamic

conditions for fabrication of both short (<10 cm) and long (>1m) monoPLOT columns and the effect of light intensity and exposure time on layer thickness in both modes was studied. The work shows that, by altering the intensity and exposure time, and through repeated exposures, it was possible to fabricate monoPLOT columns with uniform layer thicknesses ranging from <100 nm to several micrometers. The longitudinal homogeneity of the obtained polymeric stationary phases was characterized using a nondestructive (sC4D) technique.

## **EXPERIMENTAL SECTION**

Butyl methacrylate (BuMA), ethylene dimethacrylate (EDMA), 1-decanol, benzophenone, trimethoxysilylpropyl methacrylate, NaOH, and UV-initiator dimethoxy-2-phenylacetophenone

(DAP) were all purchased from Sigma–Aldrich (Gillingham, U.K.). All solvents that were used for the synthesis and washing of prepared monoliths, such as methanol (MeOH), acetone, and toluene were purchased from Lab Scan (Gliwice, Poland) and the deionized water purified by a Milli-Q system (Millipore, Bedford, MA, USA) was also utilized during washing and preparation of the fused-silica capillary. Tefloncoated fused silica capillary of 100 µm ID and 0.375 mm outer diameter (OD) was purchased from Composite Metal Services, Ltd. (Charlestown, U.K.).

Capillaries were filled with monomer mixture and washed with MeOH using a KDS-100-CE syringe pump (KD Scientific, Inc., Holliston, MA, USA). The same syringe pump was also used during capillary silanization and pretreatment. Capillary pretreatment with benzophenone was carried out using a XL-1000 Spectrolinker (Spectroline, Westbury, NY, USA). The monomer mixture was polymerized using an in-house designed purpose built prototype UV column curing device (patent application GB1109528.8, Capillary Column

Curing System, with patent authors D. Collins, E. Nesterenko, B. Heery, and B. Paull). The device feeds capillary through a chamber, which contains several circular arrays of UV LEDs at 365 nm (Figure 1). At each end of the chamber are a set of motor-driven guide rollers, which draw the capillary through the chamber.

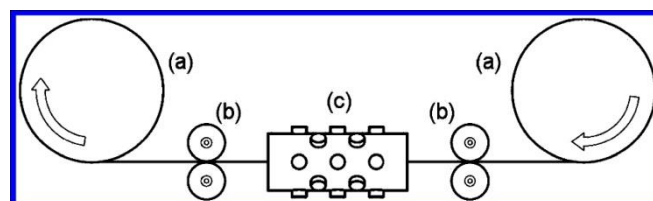


**Figure 1.** Schematic diagram of flow-through UV reactor showing (a) capillary reels, (b) guide rollers, and (c) UV chamber.

The guide rollers are driven by a stepper motor, allowing positional and speed control for the precise metering of UV radiation to the capillary. For the evaluation of column longitudinal homogeneity, both before and after polymerization, a TraceDec capacitively coupled contactless conductivity detector (C<sup>4</sup>D) (Innovative Sensor Technology GmbH, Strasshof, Austria) was used. Settings for scanning the column were as follows: frequency, 3X HIGH; voltage, -6 dB; gain, 50% and offset, 0. For the data acquisition TraceDec Monitor V. 0.07a software (Innovative Sensor Technology GmbH, Strasshof, Austria) was used. A SputterCoater 5150B (BOC Edwards, Sussex, U.K.) was utilized for coating the monoPLOT sample with a 60-nm gold layer prior to characterization using scanning electron microscopy (SEM), which was performed with a S-3400N instrument (Hitachi, Maidenhead, U.K.).

The fused-silica capillaries used for the fabrication of the monoPLOT columns were initially pretreated through activation of the surface silanol groups using sequential flushing with 1 M NaOH, deionized water, 0.1 M HCl, deionized water at a flow rate of 60  $\mu\text{L}/\text{h}$  for 2 h each, and acetone at the same flow rate for 1 h. The pretreated capillary was silanized using a 50 wt % solution of trimethoxysilylpropyl methacrylate in toluene at 60  $^{\circ}\text{C}$  for 24 h. In order to facilitate the formation of a more uniform layer, each capillary was further treated with benzophenone to introduce a layer of free radicals on the inner surface of the capillary. For this, a solution of 50 mg of benzophenone in 1 mL of MeOH prepared. The mixture was vortexed and deoxygenated under a flow of nitrogen for 10 min. The desired length of 100  $\mu\text{m}$  ID for the silanized capillary was then filled with the mixture and exposed to 1  $\text{J}/\text{cm}^2$  of UV radiation at 254 nm. The capillary then was washed with MeOH for 30 min at 3  $\mu\text{L}/\text{min}$ .

The monomer mixture used consisted of 24 wt % BuMA, 16 wt % EDMA, 60 wt % 1-decanol, and 0.4 wt % dimethoxy-2-phenylacetophenone (DAP), with respect to monomers. The mixture was prepared by first weighing out the initiator (DAP) into the mixture vessel, then adding the porogen, and last the monomers.

The mixture was then vortexed and deoxygenated under a flow of nitrogen for 10 min. The desired length of 100-  $\mu\text{m}$  ID silanized capillary was then filled with the monomer mixture and the ends of the capillary were sealed with rubber septums.

The filled capillary was loaded into the flow-through UV reactor, the capillary was aligned in the UV chamber, and the speed and intensity settings on the device were set to the desired values. For static tests, the capillary was kept stationary and was exposed to the desired amount of UV radiation through timed exposures and irradiation intensity variation.

For dynamic tests and fabrication of monoPLOT columns, the UV LEDs were first switched on and then the capillary was fed at a fixed rate through the UV chamber, the linear rate being chosen to give the desired exposure time. For multiple exposures, the capillary was passed through the chamber by the required number of exposures. After each pass, the feed motor was reversed once the end of the capillary was reached and the next exposure would be started. This was repeated for the desired number of exposures. Once the desired number of exposures had been performed, the capillary was drawn out from the UV chamber and both ends of the capillary were removed—the last few centimeters of capillary at each end received higher doses of radiation, because of the way the capillary is loaded into the device, and so it was necessary to remove these sections. Post-curing, the resultant monoPLOT column was washed with MeOH at 1  $\mu\text{L}/\text{min}$  to remove residual porogen and unreacted monomers.

## ■ RESULTS AND DISCUSSION

There has been many studies devoted to the mechanism of the formation of polymer phases within PLOT columns.<sup>27-29</sup> Various parameters, such as surface-to-volume ratio, polymerization kinetics, surface tension at the capillary inner wall, and wettability with the polymerization mixture affect the formation of the monolith in capillaries with ID < 10  $\mu\text{m}$ , resulting in deviation from the bulk porous structure and leading to the formation of PLOT columns.

Within a fused-silica capillary, particularly in which the inner surface has been pretreated with initiator, polymer growth is thermodynamically favored to occur from the capillary wall inward. This is even more so with UV-initiated polymerization, because light intensity will decrease radially toward the center of the capillary. Where polymerization conditions are limited by either time or dynamic flow, a porous layer structure results, rather than complete polymerization throughout the capillary. Early attempts to produce photoinitiated monoPLOT columns<sup>26</sup> were conducted using simple silanization of only the capillary walls with trimethoxysilylpropyl methacrylate. Although showing promising results, this approach would often result in a nonuniform layer thickness or areas of the capillary wall, where little or no polymerization would occur. This can be seen in Figure 2a.

For columns with a thicker polymer layer, this problem was more pronounced and clearly visible. In the production of PLOT columns, it is important that homogeneity is maintained as the layer thickness increases.

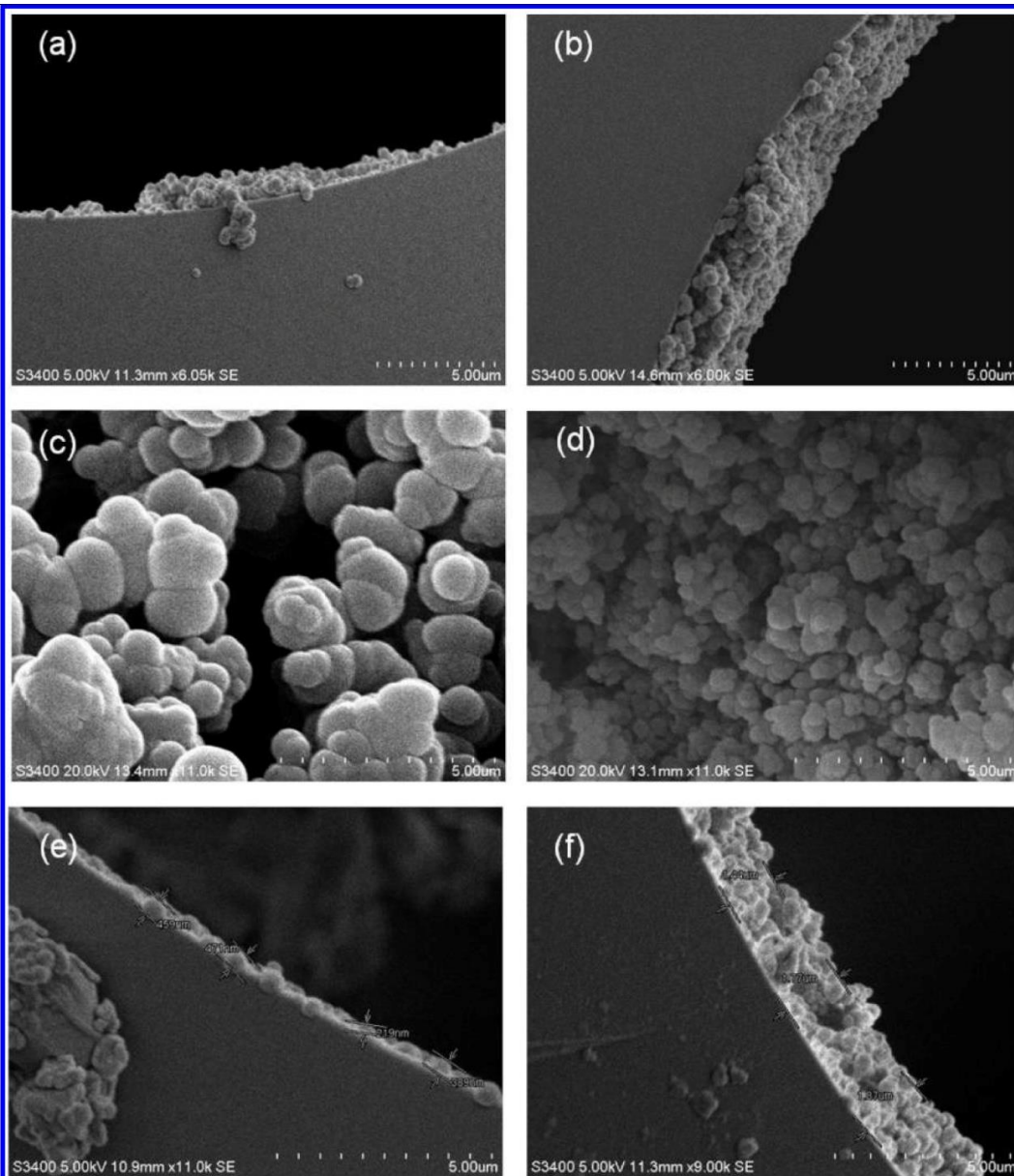


**Figure 2.** SEM images of a polymer layer formed (a) on a silanized surface and (b) on a silanized surface also treated with benzophenone. SEM images showing the different morphology of the polymer monolith layer at two different power settings: (c) 2 mW and (d) 7 mW. SEM images of the monoPLOT layer prepared via UV irradiation at (e) 6 mW for 18 s and (f) 7 mW for 18 s.

If the layer does not grow at the same rate around its circumference, the thicker regions will continue to grow at a faster rate than the rest of the layer, which can eventually result in a partially blocked column or structural weakness within the monolith. Because of side reactions, such as recombination, and inefficient synthesis of the radical species, chain reaction initiation never occurs 100% efficiently. Therefore, to increase the efficiency of the initiation reaction, by reducing the probability of side reactions at the initiation step, and in order to provide more uniform layer growth, the capillary pretreatment steps were altered to include the grafting of benzophenone, a radical polymerization initiator, directly onto the surface.

This addition ensured initiation of the polymerization reaction with equal probability along and around the inner walls of the capillary column. For comparison, two sample monoPLOT

columns were prepared under similar conditions; however, one column was subjected to a benzophenone pretreatment, while the second one was only silanized. As expected, and as shown within Figure 2b, pretreatment with benzophenone resulted in the formation of a far more uniform monolithic layer. The effects of light intensity and exposure time were investigated in a series of static tests. It is known that the kinetics of the UV initiated reaction (and, as a result, its speed) is dependent on the light intensity.<sup>30</sup> The classical equation for the polymerization rate is given as

$$R_p = \frac{k_p}{k_t^{0.5}} [M] \left( \frac{R_i}{2} \right)^{0.5}$$

where [M] is the concentration of monomer,  $R_i$  is the initiation rate,  $k_p$  and  $k_t$  are the propagation and termination rate coefficients, respectively. However, in the case of photoinitiated reactions, the above equation takes the form

$$R_p = \frac{k_p}{k_t^{0.5}} [M] (\Phi I_a)^{0.5}$$

or

$$R_p = \frac{k_p}{k_t^{0.5}} [M] \{ \Phi I_0 [1 - \exp(-\epsilon [In] b)] \}^{0.5}$$

where  $\Phi$  is the quantum yield for initiation,  $I_a$  the absorbed light intensity,  $I_0$  the incident light intensity,  $\epsilon$  the extinction coefficient, [In] the photoinitiator concentration, and  $b$  the layer thickness.

It can be seen from eq 3 that the rate is directly proportional to the light intensity  $I_a$ . Initial studies were carried out to determine the useful operating limits of the device, with respect to the intensity setting of the UV LEDs and the exposure time to which the capillary was subjected. These limits were determined through fabricating monolithic layers within 100  $\mu$ m ID capillary, varying both UV light intensity and exposure time. The UV LEDs used had a minimum forward voltage of 3.08 V and a current draw of 20 mA. For this type of LED, the optical output power can be approximated as  $1/10$ th of the forward current, so the minimum chamber power was  $\sim 2$  mW. It was found that the optimum range for chamber power was 5–7 mW. At low power settings, below 4 mW, polymerization was very slow and the resulting layer was very fragile.

Above 7 mW, polymerization occurred at such a fast rate that it was almost impossible to control it, making the fabrication of a uniform layer extremely difficult. It was also observed that fabrication at high power settings often resulted in partial or complete overpolymerization of the capillary. It was found that the morphology of the polymer layer can also be varied through the adjustment of the UV light intensity. Thus, at 2 mW,



polymerization was extremely slow and the resultant polymer layer exhibited larger pore sizes, namely,  $1.25 \pm 0.38 \mu\text{m}$  (measured from SEM images, sample number,  $n = 15$ ) and a less-uniform structure (see Figure 2c).

However, the use of higher power settings provided the formation of pores of smaller dimensions:  $0.68 \pm 0.17 \mu\text{m}$  at 6 mW, and  $0.47 \pm 0.16 \mu\text{m}$  at 7 mW (Figure 2d). This shows that the UV light intensity has an effect on polymerization thermodynamics similar to that of temperature in thermally initiated polymerization, where the reaction rate is slower at lower temperature and increases with higher temperature.<sup>31</sup> First, the initiation rate in the case of nonchain initiator decay is proportional to the efficiency of the initiator ( $f$ , which is usually between 0.5 and 1.0), the constant of the initiator decay ( $k_d$ ), and the initiator concentration  $[In]$ :

$$R_i = 2fk_d[In]$$

However, the rate of polymerization is dependent on light intensity (eq 3), providing higher polymerization rate at higher intensity. Since the formation of new polymerization centers is faster than the growth of globules, the supply of monomers runs low more rapidly and the number of globules is large, but their size remains small, which leads to smaller voids between globules. Two sample SEM images showing the layers formed at two different power settings but with the same exposure time are also shown in Figures 2e and 2f.

The difference in layer thickness is clear; however, it was also possible to see a variation in the morphology of the polymer layer, with a larger globule and pore size for the 6 mW exposure (Figure 2e), compared to the higher power 7-mW exposure (Figure 2f). The next experiments were carried out to measure the average thickness of the monolith layer at increasing exposure times, and this was performed at three different power settings between 5 and 7 mW. Exposure times were varied from 7 s to 25 s.

For each monoPLOT column fabricated under a particular condition, the layer thickness was determined from SEM images. Figure 4a shows the relationship between exposure time and layer thickness for different power and time settings. It can be seen that the thickness of the polymer layer grows exponentially with time. Such behavior can be explained from consideration of reaction kinetics. Equation 3 shows that the rate of the reaction is dependent on the layer thickness  $b$ ; thus, the thicker the layer, the more negative the exponent value becomes, and, as a result, the reaction rate increases.

However, the variation in layer thickness homogeneity also increases at higher exposure times and with increasing intensity of the incident light. This creates a problem, because, in order to achieve the optimum morphology in the polymer layer, it is necessary to polymerize within this given intensity range; however the rate of polymer growth at these intensities is extremely high, and, therefore, control of exposure time must be very precise.

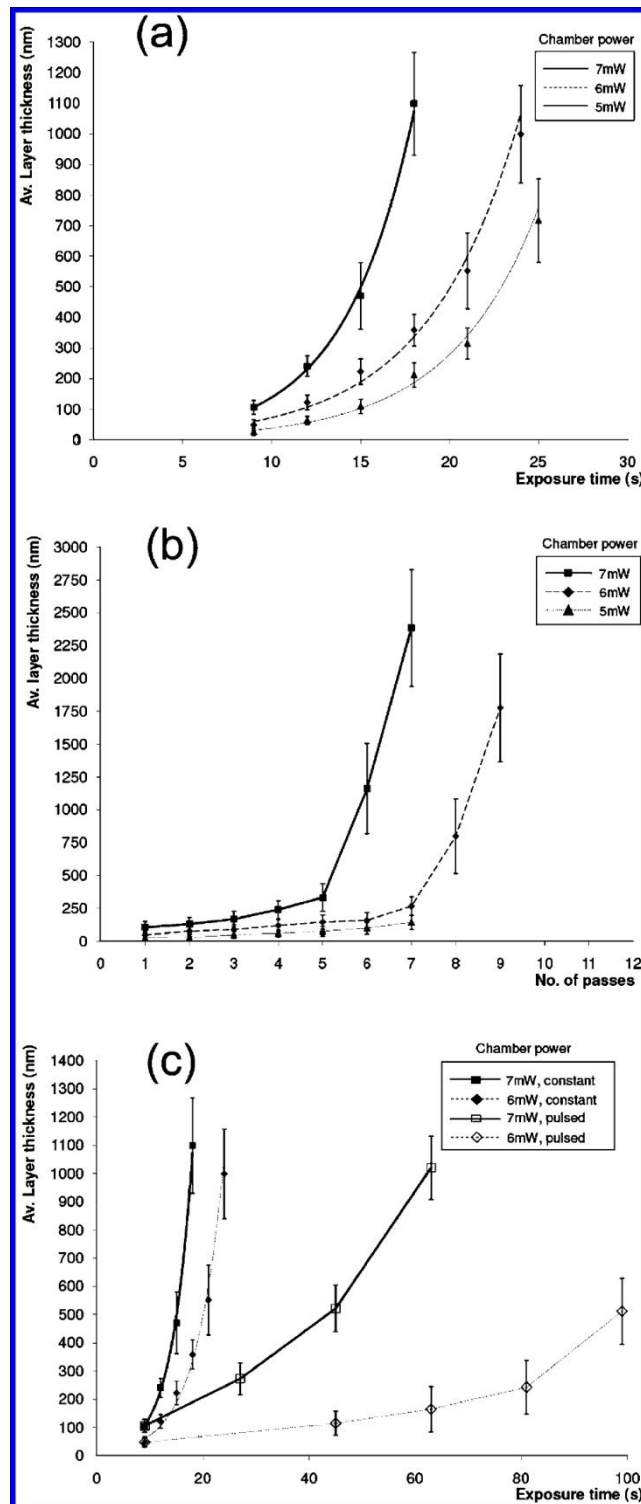


**Figure 4.** (a) Plot of average layer thickness against exposure time for power settings of 5, 6, and 7 mW. (b) Comparison of layer thickness for multiple exposures (passes) at 5, 6, and 7 mW for dynamic tests. (c) Comparison of layer thickness at two different power levels, 6 and 7 mW, for both continuous and 9-s multiple exposures.

The developed approach to column fabrication was readily amenable to both flow-through polymerization and timed exposure experiments. Therefore, to investigate the possibility to more precisely control monoPLOT layer formation (without changing the composition of the monomer mixture), two new polymerization approaches were investigated using the device.

These were (1) pumping the monomer mixture through the capillary during polymerization, "flow-through polymerization", and (2) multiple exposures, irradiating the monomer filled capillary with several repeated short exposures. Flow-through polymerization was investigated as an approach, because the liquid flow would remove short polymer chains and supply fresh monomer mixture, facilitating polymerization specifically on the sites that are already attached to the capillary walls, providing more-uniform layer growth. The monomer mixture was pumped through the capillary at a fixed flow rate of 1 /4L/min, corresponding to a linear velocity of 2.1 mm/s in a 100- $\mu$ m capillary. This low flow rate was chosen to minimize any damage to the monolithic layer forming during polymerization by other polymerized particles that could be caught in the flowing stream. It was observed that flow-through polymerization greatly reduced the rate of growth of the polymer layer, giving a more linear relationship between exposure time and layer thickness. Comparative images for monoPLOT columns prepared in flow-through and static conditions can be seen in Figures 3a and 3b, respectively. The columns produced under flow-through conditions were exposed to UV light at 7 mW for 65 s, receiving a total dosage of 455 mJ. However, static exposure to 455 mJ would result in complete polymerization across the capillary. The column produced under static conditions was exposed to light, also at 7 mW, but for just 13 s, giving a dosage of 91 mJ. The average layer thickness for the column prepared by flow-through polymerization was 332 nm, whereas for the static approach, it was 1.4  $\mu$ m.

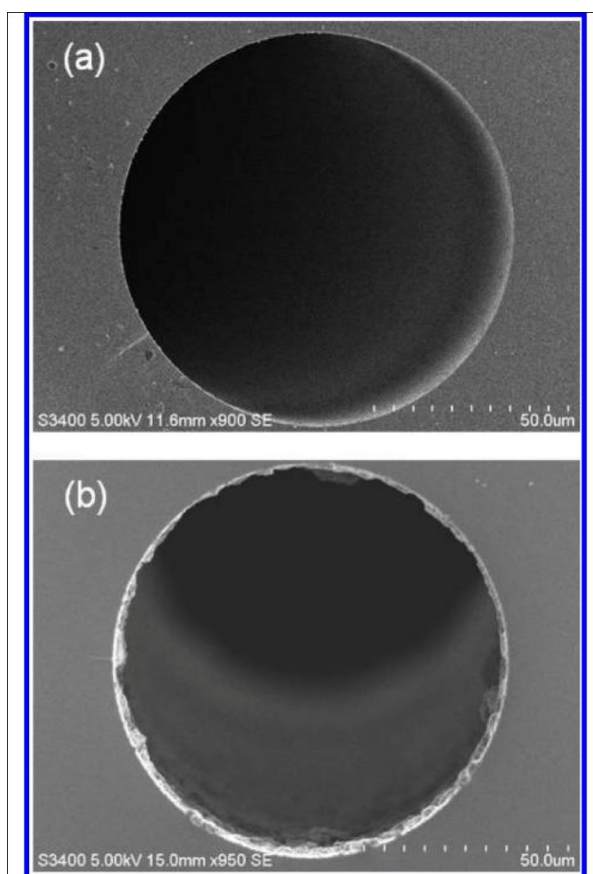


**Figure 3.** Comparison of two monoPLOT columns polymerized under (a) static and (b) flow-through conditions.

It is worth noting that the flow-through approach produced a polymer layer, which, although thinner, was extremely uniform along the length and circumference of the column. It is also worth noting here that the monomer mixtures used in both the static and flow-through polymerization were identical. In both instances, the monomers were used without removal of any polymerization inhibitors; as such, the changes in the rate of polymerization observed could only be attributed to the physical differences in the polymerization process using the two approaches.

One of the advantages of the photoinitiated polymerization is the ability to initiate and halt the reaction relatively rapidly, compared to thermally initiated polymerization approaches.<sup>3°</sup> Applying this approach, in which radicals are generated over short periods of time, it was hoped that this situation would facilitate a more controlled polymerization process and thus allow the fabrication of a more homogeneous layer. For multiple exposures, the polymerization mixtures were similar to those discussed previously during static testing. However, in this instance, the full dose of radiation would be delivered in smaller discrete doses, thus controlling the duration of the reaction. Since the minimum draw speed of the device was 7.2 mm/s and the chamber length was 65 mm this gave a minimum dynamic exposure time of —9 s.

In order to record useful data at parameters that could be further used in dynamic testing, it was decided to use 9 s as the exposure time for each dose of UV energy. For the static study, a length of capillary was filled with a monomer mixture, as done previously, and aligned within the UV chamber. The polymerization study, as described earlier, was repeated for three power settings; 5, 6, and 7 mW. However, in this case, the dose of radiation was given in 9 s doses, and the number of doses was varied. The resultant polymer layers were inspected and their thickness was measured as done previously, using SEM. A comparison of constant exposures against multiple short exposures (passes) for chamber powers of 6 and 7 mW is shown in Figure 4b. It can be seen that, for a given total energy supplied, the rate of polymer growth for multiple exposures was considerably slower and therefore more controlled. In addition, when contrasted to the data shown in Figure 4a, it can be seen that the variation in layer thickness is also much lower, compared to long single exposures.

Using the results obtained from the above static tests, it was possible to determine the range of best parameters for dynamic tests and for polymerization of longer monoPLOT capillary columns. Therefore, a length of pretreated capillary was filled with monomer mixture, and its ends were capped, and then the capillary fed into the UV reactor. For dynamic studies, the capillary was exposed to UV radiation while, at the same time, being drawn through the UV chamber at a fixed speed. In this case, the linear speed was set to its minimum value of 7.2 mm/ s, giving each unit length of capillary an exposure time of 9 s for each pass. At a power setting of 7 mW, this corresponds to 63 mJ of energy per pass. A setting of 6 mW will yield 54 mJ per pass, and 5 mW will give 45 mJ.

The results of this dynamic study can be seen in Figure 4c. It was interesting to observe that the layer thicknesses obtained were considerably thicker compared to static tests, which were carried out under the same conditions and indicated that there was a far higher rate of

polymer growth with longer capillaries. The reason for the increased rate of polymer growth is assumed to be from light scattering within the capillary. The propagation of light through fused-silica capillaries has already been well-documented,<sup>25,32</sup> and it has been shown that the capillary can transmit a considerable amount of light along its length. During dynamic fabrication, the capillary was exposed to some UV radiation before being drawn into the UV chamber, because of light propagation along the capillary. The same effect will also be present on the other side of the UV chamber, where the post-exposure capillary was also further irradiated.

This results in an overall thicker polymer layer, because the total dosage per unit length is higher. As part of the dynamic study, several long monoPLOT columns were formed, with lengths ranging from 300 mm to 1750 mm. All of these columns were characterized using sC4D, which is known to be a nondestructive technique for the characterization of capillary stationary phases,<sup>33</sup> and several were further evaluated via SEM analysis. The layer thickness measurements and homogeneity of one such 300-mm example is presented in Figure 5a. The layer thickness was determined from the SEM images of the cross sections of the monoPLOT column.

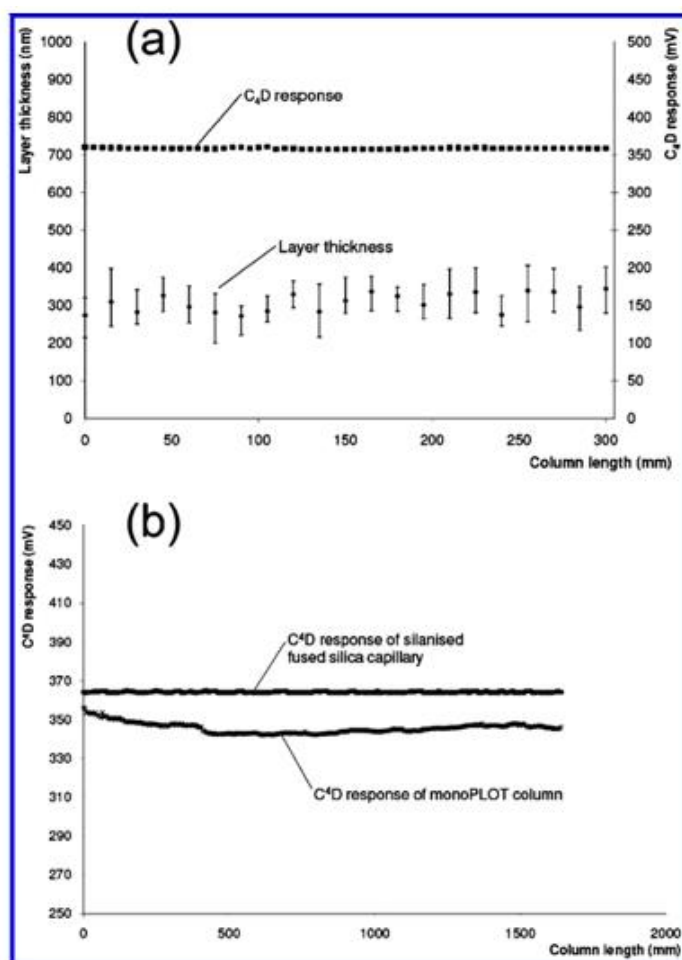


Figure 5. (a) Layer thickness and sC<sub>4</sub>D characterization of a 300-mm column produced over five exposures at 7 mW. (b) sC<sub>4</sub>D characterization comparison between a 1750-mm monoPLOT column produced over five exposures at 7 mW and a silanized silica capillary. Capillary feed rate was 7.2 mm/s, giving an exposure time of ~9 s.

For this, a 300-mm-long monoPLOT column (after sC<sup>4</sup>D scan) was cut into thirty 10-mm-long sections and the layer thickness was measured from the SEM images (n = 30). Although layer thickness measurements were intermittent, it can be seen that the average thickness of the polymer layer is ~310 nm and it is consistent along the column. At the same time, the sC<sup>4</sup>D scan showed that the layer was homogeneous (sC<sup>4</sup>D RSD of 0.22%) and confirmed that there were no voids or blockages along the length of the column. Further work yielded a 1750-mm column and the sC<sup>4</sup>D characterization of this column is shown in Figure 5b. The relative standard deviation (RSD) of layer thickness for this column is 0.78%. A 10-mm segment from the end of the column was removed and was further inspected via SEM, showing the resultant polymer layer to be very uniform with an average layer thickness of ~400 nm.

## ■ CONCLUSIONS

The results presented within this work demonstrate a new technology and approach for the precise fabrication of monoPLOT columns of controlled layer thickness and length. The fine control of the monolith morphology and the formation of polymer layers have been demonstrated at several intensities of 365-nm ultraviolet (UV) light and at various exposure times. The relationship between exposure time and layer thickness at different intensities was investigated and clarified. The application of multiple exposures and of flow-through polymerization was also investigated and optimum conditions for the fabrication of long monoPLOT columns were established. Again, the relationship between layer thickness and exposure time for multiple exposures was also plotted, as were the results of flow-through polymerization. The columns obtained during static and dynamic fabrication were further inspected through scanning capacitively coupled contactless conductivity detection (sC<sup>4</sup>D) characterization, showing excellent homogeneity of the polymer layer along the length of the columns. This novel method opens up many more possibilities for the fabrication of monoPLOT columns and provides some interesting insights into the polymerization process and the various user-controlled effects that can be employed during polymerization.

## ■ ACKNOWLEDGMENTS

The authors would like to acknowledge financial support from Science Foundation Ireland for the Irish Separation Science Cluster award (Grant No. 08/SRC/B1412).

## ■ REFERENCES

- (1) Golay, M. J. E. In *Gas Chromatography*; Coates, V. J., et al., Ed.; Academic Press: New York, 1958; pp 1-13.
- (2) de Zeeuw, J. *LC-GC Eur.* 2011, 24, 38-45.
- (3) Eeltink, S.; Svec, F.; Frechet, J. M. J. *Electrophoresis* 2006, 27, 4249-4256.

- (4) Yu, C.; Svec, F.; Frechet, J. M. T. *Electrophoresis* 2000, 21, 120-127.
- (5) Zaidi, A.; Cheong, W. T. *Electrophoresis* 2009, 30, 1603-1607.
- (6) Chen, J. L.; Lin, Y. C. T. *Chromatogr. A* 2010, 1217, 4328-4336.
- (7) Bakry, R.; Gjerde, D.; Bonn, G. K. T. *Proteome Res.* 2006, 5, 1321-1331.
- (8) Hirayama, Y.; Ohmichi, M.; Tatsumoto, H. J. *Health Sci.* 2005, 51, 526-532.
- (9) Niessen, W. M. A.; Poppe, H. T. *Chromatogr.* 1985, 323, 37-46.
- (10) Escoffier, B. H.; Parker, C. E.; Mester, T. C.; Dewit, J. S. M.; Corbin, F. T.; Jorgensen, J. W.; Tomer, K. B. J. *Chromatogr. A* 1989, 474, 301-316.
- (11) Swart, R.; Kraak, J. C.; Poppe, H. *TrAC Trends Anal. Chem.* 1997, 16, 332-242.
- (12) Yue, G.; Luo, Q.; Zhang, J.; Wu, S. L.; Karger, B. L. *Anal. Chem.* 2007, 79, 938-946.
- (13) Rogeberg, M.; Wilson, S. R.; Greibrokk, T.; Lundanes, E. J. *Chromatogr. A* 2010, 1217, 2782-2786.
- (14) Wang, D.; Hincapie, M.; Rejtar, T.; Karger, B. L. *Anal. Chem.* 2011, 83, 2029-2037.
- (15) Causon, T. J.; Shellie, R. A.; Hilder, E. F.; Desmet, G.; Eeltink, S. T. *Chromatogr. A* 2011, 1218, 8388-8393.
- (16) Abi Jaoude, M.; Randon, J. *Anal. Bioanal. Chem.* 2011, 400, 1241-1249.
- (17) Yang, L.; Guihen, E.; Holmes, J. D.; Loughran, M.; O'Sullivan, G. P.; Glennon, J. D. *Anal. Chem.* 2005, 77, 1840-1846.
- (18) de Zeeuw, J.; de Nijs, R. C. M.; Buyten, J. C. J.; Peene, A.; Mohnke, M. T. *High Res. Chromatogr.* 1988, 11, 162-167.
- (19) Ruan, Z.; Liu, H. T. *Chromatogr. A* 1995, 693, 79-88.
- (20) Luo, Q.; Yue, G.; Valaskovic, G. A.; Gu, Y.; Wu, S. L.; Karger, B. L. *Anal. Chem.* 2007, 79, 6174-6181.
- (21) Luo, Q.; Ge, Y.; Wu, S. L.; Rejtar, T.; Karger, B. L. *Electrophoresis* 2008, 29, 1604-1611.
- (22) Luo, Q.; Wu, S. L.; Rejtar, T.; Karger, B. L. *J. Chromatogr. A* 2009, 1216, 1223-1231.
- (23) Xu, L.; Sun, Y. *Electrophoresis* 2008, 29, 880-888.
- (24) Kuban, P.; Dasgupta, P.; Pohl, C. A. *Anal. Chem.* 2007, 79, 5462-5467.
- (25) Abele, S.; Smejkal, P.; Yavorska, O.; Foret, F.; Macka, M. *Analyst* 2010, 135, 477-481.
- (26) Nesterenko, E.; Yavorska, O.; Macka, M.; Yavorsky, A.; Paull, B. *Anal. Methods* 2011, 3, S37-543.
- (27) Nischang, I.; Svec, F.; Frechet, J. M. J. *Anal. Chem.* 2009, 81, 7390-7396.
- (28) He, M.; Zeng, Y.; Sun, X. J.; Harrison, D. J. *Electrophoresis* 2008, 29, 2980-2986.
- (29) Nischang, I.; Brueggemann, O.; Svec, F. *Anal. Bioanal. Chem.* 2010, 397, 953-960.
- (30) Andrzejewska, E. *Prog. Polym. Sci.* 2001, 26, 605-665.
- (31) Svec, F.; Tennikova, T. B.; Deyl, Z. *J. Chromatogr. Libr.* 2003, 19-50.
- (32) Piasecki, T.; Macka, M.; Paull, B.; Brabazon, D. *Opt. Lasers Eng.* 2011, 49, 924-931.
- (33) Gillespie, E.; Connolly, D.; Macka, M.; Nesterenko, P. N.; Paull, B. *Analyst* 2007, 132, 1238-1245.